

Extrinsic Total-Variance and Coplanarity via Oriented and Classical Projective Shape Analysis

Musab Alamoudi* Robert L. Paige[†] Vic Patrangenaru[‡]

November 18, 2025

Abstract

Projective shape analysis provides a geometric framework for studying digital images acquired by pinhole digital cameras. In the classical projective shape (PS) method, landmark configurations are represented in $(\mathbb{RP}^2)^{k-4}$, where k is the number of landmarks observed. This representation is invariant under the action of the full projective group on this space and is sign-blind, so opposite directions in \mathbb{R}^3 determine the same projective point and front-back orientation of a surface is not recorded. Oriented projective shape (OPS) restores this information by working on a product of $k-4$ spheres \mathbb{S}^2 instead of projective space and restricting attention to the orientation-preserving subgroup of projective transformations. In this paper we introduce an extrinsic total-variance index for OPS, resulting in the extrinsic Fréchet framework for the m dimensional case from the inclusion $j_{\text{dir}} : (\mathbb{S}^m)^q \hookrightarrow (\mathbb{R}^{m+1})^q$, $q = k - m - 2$. In the planar pentad case ($m = 2$, $q = 1$) the sample total extrinsic variance has a closed form in terms of the mean of a random sample of size n of oriented projective coordinates in S^2 . As an illustration, using an oriented projective frame, we analyze the Sope Creek stone data set, a benchmark and nearly planar example with 41 images and 5 landmarks. Using a delta-method applied to a large sample and a generalized Slutsky theorem argument, for an OPS leave-two-out diagnostic, one identifies coplanarity at the 5% level, confirming the concentrated data coplanarity PS result in Patrangenaru(2001)[11].

Key words. oriented projective shape, extrinsic total variance, nonparametric coplanarity test, directional statistics, statistical image analysis.

MSC2020: 62R30, 62H35, 62H15

*King Abdulaziz University, Jeddah, P.O. Box 80200, Zip Code 21589, Kingdom of Saudi Arabia.

[†]Department of Mathematics and Statistics, Missouri University of Science and Technology, Rolla, MO 65409, U.S.A.

[‡]Department of Statistics, Florida State University, Tallahassee, FL 32304, U.S.A, vic@stat.fsu.edu.

1 Introduction

Landmarked images obtained from pinhole cameras or similar optical systems can be studied using projective geometry. Three-dimensional scenes are mapped to the image plane by a central projection, and projective shape analysis studies the resulting landmark configurations modulo projective transformations (see Patrangenaru and Ellingson [9] and references therein). In the classical projective shape (PS) model, configurations are represented in $(\mathbb{RP}^m)^q$ and are invariant under the full projective group $\text{PGL}(m+1, \mathbb{R})$.

A basic feature of this model is that it is insensitive to the sign of homogeneous coordinates: the projective point $[x] \in \mathbb{RP}^m$ identifying the real and virtual directions x and $-x$ in \mathbb{R}^{m+1} . For many applications this is appropriate, but in situations where a physical surface has a natural orientation, such as a rock face, a biological surface, or a road scene, the difference between front and back is meaningful. In such settings, oriented projective geometry and oriented projective shape (OPS) provide a more faithful description [6, 12].

The OPS framework replaces axes by directions on the unit sphere \mathbb{S}^m and restricts attention to orientation-preserving transformations $\text{OPGL}(m)$. Choi et al(2022)[12] defined OPS shape spaces, and represented them as products $(\mathbb{S}^m)^q$ of spheres, thus allowing for a extrinsic or intrinsic Fréchet analysis on these spaces, linking OPS analysis with multivariate directional statistics.

The present paper focuses on *extrinsic total variance* in the OPS case, aiming to measure and test for the overall dispersion of oriented projective coordinates. The motivating hypothesis is coplanarity: if a landmarked surface is flat, then after OP coordinate representation relative to a fixed oriented projective frame from the landmark configuration, the OP coordinates of the remaining landmarks configuration should be constant, thus their OPS total variance should vanish.

We extend work in the extrinsic Fréchet framework in Patrangenaru and Ellingson [9], using the inclusion

$$j_{\text{dir}} : (\mathbb{S}^m)^q \hookrightarrow (\mathbb{R}^{m+1})^q$$

and the usual Euclidean distance in the ambient numerical space. In the planar single- OP coordinate case ($m = 2, q = 1$), the resulting OPS total-sample variance index turns out to have a particularly simple form:

$$tS_{n,\text{OPS}} = 2(1 - R_n), \quad R_n = \|\bar{u}\|,$$

where \bar{u} is the sample mean of the OPS unit vectors representing the oriented OP coordinates of the sample of size n of k -ads . This expression mirrors the Veronese–Whitney (VW) PS total sample variance $2(1 - \lambda_1^{(n)})$ based on the largest eigenvalue of the mean of the empirical in the space of symmetric matrices (see Fisher et.al.(1996)[5]).

Our approach is as follows: (i) we define the population OPS total-variance $t\Sigma_{\text{OPS}}$ and its sample counterpart $tS_{n,\text{OPS}}$ using an extrinsic Fréchet framework, (ii) using a delta-method we derive the standard error and large-sample confidence intervals for $t\Sigma_{\text{OPS}}$; (iii) we find confidence intervals for $t\Sigma_{\text{OPS}}$, using both the chi-square and normal-approximations for the

distribution of $tS_{n,OPS}$; (iv) using large sample theory, we test for the coplanarity of the Sope Creek landmark data via the hypothesis $H_0 : t\Sigma_{OPS} = 0$. The results confirm and extend those in Patrangenaru [11], that were restricted to a small support of data assumption.

Section 2 reviews projective and oriented projective shape. Section 3 introduces the OPS extrinsic total-variance index and its asymptotic variance. Here one recalls the VW PS total variance formulas. Section 4 formulates the OPS coplanarity test and leave-two-out diagnostic and presents the Sope Creek stone analysis. A short discussion appears in Section 5.

2 Projective and Oriented Projective Shape

In this section, following Mardia and Patrangenaru(2005)[6] and Choi et al(2022)[12] we briefly recall definitions of projective shape and oriented projective shape. We focus on the planar case $m = 2$ and a single remaining landmark, in view of our application.

2.1 Projective shape and its representation via projective frames

Points in a numerical space are here presented as column vectors. Given $k \geq m + 2$, a k -ad in \mathbb{R}^m is an ordered set of labeled points (x_1, \dots, x_k) in \mathbb{R}^m . To each point $x \in \mathbb{R}^m$, we associate the projective point $[\tilde{x}] \in \mathbb{R}P^m$, where

$$\tilde{x} = (x^T, 1)^T \in \mathbb{R}^{m+1}$$

A *projective frame*(or *projective basis*) in an m dimensional real projective space is an ordered set of $m + 2$ projective points in general position. An example of projective frame is the *standard projective frame* is $([e_1], \dots, [e_{m+1}], [e_1 + \dots + e_{m+1}])$ in $\mathbb{R}P^m$.

In projective shape analysis it is preferable to employ coordinates invariant with respect to the group $PGL(m + 1)$ of projective transformations of $\mathbb{R}P^m$. Recall that we define an element of $\beta = \beta_A \in PGL(m + 1)$ given in terms of a matrix $A \in GL(m + 1)$, defined by its action on $\mathbb{R}P^m$ as follows: $\beta([x]) = [Ax]$. The projective transformation takes a projective frame to a projective frame, and its action on $\mathbb{R}P^m$ is determined by its action on a projective frame, therefore we define the *projective coordinate(s)* of a point $p \in \mathbb{R}P^m$ w.r.t. a projective frame $\pi = (p_1, \dots, p_{m+2})$ as being given by

$$p^\pi = \beta^{-1}(p), \quad (1)$$

where $\beta \in PGL(m+1)$ is the unique projective transformation taking the standard projective frame to π . These coordinates automatically have the projective invariance property.

Remark 2.1. Assume u, u_1, \dots, u_{m+2} are points in \mathbb{R}^m , such that $\pi = ([\tilde{u}_1], \dots, [\tilde{u}_{m+2}])$ is a projective frame. If we consider the $(m + 1) \times (m + 1)$ matrix $U_m = [\tilde{u}_1^T, \dots, \tilde{u}_{m+1}^T]$, the projective coordinates of $p = [\tilde{u}]$ w.r.t. π are given by

$$p^\pi = [y^1(u) : \dots : y^{m+1}(u)], \quad (2)$$

where

$$v(u) = U_m^{-1} \tilde{u}^T \quad (3)$$

and

$$y^j(u) = \frac{v^j(u)}{v^j(u_{m+2})}, \forall j = 1, \dots, m+1. \quad (4)$$

A k-ad $x = (x_1, \dots, x_k)$ is said to be *in general position* if the set of labels of its points includes an ordered subset $F = \{f_1, \dots, f_{m+2}\}$ such that $\pi_F = ([\tilde{x}_{f_1}], \dots, [\tilde{x}_{f_{m+2}}])$ is a projective frame. The projective coordinates $([y_1], \dots, [y_{k-m-2}])$ of the remaining landmarks with respect to π_F , listed in the order they appear in the k-ad, give a multivariate axial representation of the projective shape of the k-ad $([\tilde{x}_1], \dots, [\tilde{x}_k])$, therefore projective shape analysis of k-ads in $P\Sigma_m^k$ is reduced to data analysis on $(\mathbb{R}P^m)^q$, $q = k - m - 2$ (see Patrangenaru and Ellingson (2015)[9])

2.2 Oriented projective shape and multivariate directional data analysis

The m dimensional *oriented projective space* $\overrightarrow{\mathbb{R}P}^m$ is the quotient $\mathbb{R}^{m+1} \setminus \{0\} / \sim$ where $x \sim y$ iff there is a positive scalar λ such that $x = \lambda y$. The equivalence class of $x \in \mathbb{R}^{m+1} \setminus \{0\}$ is an oriented projective point, labeled $\overrightarrow{[x]}$. Oriented projective geometry identifies points on rays originating from the null vector in \mathbb{R}^{m+1} . Such rays are identified with a unit vectors on the sphere

$$\mathbb{S}^m = \{x \in \mathbb{R}^{m+1} : \|x\| = 1\},$$

therefore we may identify $\overrightarrow{\mathbb{R}P}^m$ with \mathbb{S}^m . Each nonzero vector x defines a direction $x/\|x\| \in \mathbb{S}^m$. The \pm sign distinguishes now opposite directions. An *oriented projective frame* in $\overrightarrow{\mathbb{R}P}^m$ is an ordered set of $m+2$ oriented projective points in general position $(\overrightarrow{[x_1]}, \dots, \overrightarrow{[x_{m+2}]})$, such that x_{m+2} is a convex linear combination of x_1, \dots, x_{m+1} . An example of oriented projective frame is the *standard oriented projective frame* $(\overrightarrow{[e_1]}, \dots, \overrightarrow{[e_{m+1}]}, \overrightarrow{[e_1 + \dots + e_{m+1}]})$ in $\overrightarrow{\mathbb{R}P}^m$.

In OPS analysis one considers oriented k-ads. An oriented k-ad is a k-ad $(\overrightarrow{[x_1]}, \dots, \overrightarrow{[x_k]})$ that includes an oriented projective frame.

Definition 2.2. The *oriented projective group* is $OPGL(m)$, the set of projective transformations g_P , depending on matrices $P \in GL^+(m+1, \mathbb{R})$ (positive determinant), acting by $g_P(\overrightarrow{[x]}) = \overrightarrow{[Px]}$.

Note that $OPGL(m)$ acts simply transitively on oriented projective frames (see Stolfi(1991)[13]), therefore the action on $\overrightarrow{\mathbb{R}P}^m$ is determined by its action on a projective frame, thus allowing one to define the *oriented projective coordinate(s)* of a point $p \in \overrightarrow{\mathbb{R}P}^m$ w.r.t. an oriented projective frame $\pi = (p_1, \dots, p_{m+2})$ as being given by

$$p^\pi = \beta^{-1}(p), \quad (5)$$

where $\beta \in OPGL(m)$ is the unique projective transformation taking the standard oriented projective frame to π .

Remark 2.3. Assume u, u_1, \dots, u_{m+2} are points in \mathbb{R}^m , such that $\pi = ([\tilde{u}_1], \dots, [\tilde{u}_{m+2}])$ is an oriented projective frame. If we consider the $(m+1) \times (m+1)$ matrix $U_m = [\tilde{u}_1^T, \dots, \tilde{u}_{m+1}^T]$, the oriented projective coordinates of $p = [\tilde{u}]$ w.r.t. π are given by

$$p^\pi = \overrightarrow{[y^1(u), \dots, y^{m+1}(u)]}, \quad (6)$$

where

$$v(u) = U_m^{-1} \tilde{u}^T \quad (7)$$

and

$$y^j(u) = \frac{v^j(u)}{v^j(u_{m+2})}, \forall j = 1, \dots, m+1. \quad (8)$$

Fix an oriented projective frame $\pi = (p_{f_1}, \dots, p_{f_{m+2}})$ selected from an oriented k-ad and for each label $f \notin F$, find the corresponding vector $y_f = (y_f^1, \dots, y_f^{m+1}) \in \mathbb{R}^{m+1}$ using Remark 2.3. Then $w_f = \frac{y_f}{\|y_f\|} \in \mathbb{S}^m$.

Thus the OPS of the oriented k-ad, is now registered as a point

$$w \in (\mathbb{S}^m)^q,$$

where $w = (w_f)_{f \notin F}$. In what follows we work directly with the normalized coordinates $w \in (\mathbb{S}^m)^q$.

3 OPS Extrinsic Total Variance

We now define an OPS total-variance index in the extrinsic Fréchet framework, starting from the directional embedding and then specializing to the planar single-oriented projective coordinate case.

3.1 Directional embedding and extrinsic Fréchet mean

The basic idea of extrinsic Fréchet statistics is to embed the manifold of interest into a Euclidean space, perform Euclidean calculations there, and then project back to the manifold [9]. For OPS we use the inclusion map as embedding

$$j_{\text{dir}} : (\mathbb{S}^m)^q \hookrightarrow (\mathbb{R}^{m+1})^q, \quad j_{\text{dir}}(u_1, \dots, u_q) = (u_1, \dots, u_q).$$

The ambient space is $\mathbb{R}^{(m+1)q}$ with its usual Euclidean norm.

Let $U = (U^{(1)}, \dots, U^{(q)})$ be an $(\mathbb{S}^m)^q$ -valued random variable with distribution ν . The *extrinsic Fréchet function* associated with j_{dir} is

$$F_E(z) = \mathbb{E} \|j_{\text{dir}}(U) - j_{\text{dir}}(z)\|^2, \quad z \in (\mathbb{S}^m)^q.$$

Any minimizer of F_E is called an *extrinsic Fréchet mean* of U with respect to j_{dir} .

In the single oriented projective coordinate case $q = 1$ we write $U^{(1)} \in \mathbb{S}^m$ and

$$\mu = \mathbb{E}[U^{(1)}] \in \mathbb{R}^{m+1}.$$

Assuming $\mu \neq 0$, the extrinsic mean direction is obtained by projecting μ back to the sphere:

$$\mu_E = \frac{\mu}{\|\mu\|} \in \mathbb{S}^m.$$

For a sample $\{u_i\}_{i=1}^n \subset \mathbb{S}^m$ the empirical counterparts are

$$\bar{u} = \frac{1}{n} \sum_{i=1}^n u_i, \quad \hat{\mu}_E = \frac{\bar{u}}{\|\bar{u}\|}$$

provided $\bar{u} \neq 0$.

The quantity

$$R_n = \|\bar{u}\|$$

is the sample *mean resultant length* from directional statistics and lies in $[0, 1]$. It is close to 1 when the u_i are highly concentrated on the sphere and significantly smaller than 1 when the u_i are more spread out.

3.2 Population and sample total-variance indices

The extrinsic covariance matrix Σ_E of $U^{(1)}$ is given in Bhattacharya and Patrangenaru (2005) [4]. Using that closed formula, one can easily show that when $q=1$, the population OPS extrinsic total-variance is

$$t\Sigma_{\text{OPS}} = 2(1 - R) = 2\left(1 - \|\mathbb{E}[U^{(1)}]\|\right).$$

The OPS extrinsic total variance vanishes if and only if $U^{(1)}$ is almost surely constant, and increases as the distribution of $U^{(1)}$ spreads out on the sphere.

Given an OPS random sample of oriented $(m+3)$ -ads in their spherical representation $\{u_i\}_{i=1}^n \subset \mathbb{S}^m$, the sample OPS extrinsic total variance is

$$tS_{n,\text{OPS}} = 2(1 - R_n), \quad R_n = \|\bar{u}\|. \quad (9)$$

In the Sope Creek application we have $m = 2$ and $q = 1$, so (9) completely describes the OPS total variance in terms of the mean of the three-dimensional unit vectors $\{u_i\}$.

3.3 VW total-variance and VW mean axis

For a comparison we review the extrinsic total-variance index in the PS model based on the Veronese–Whitney embedding. For $[x] \in \mathbb{RP}^m$ with $x \in \mathbb{R}^{m+1} \setminus \{0\}$, the Veronese–Whitney embedding is defined by

$$j_{\text{VW}}([x]) = \frac{xx^\top}{\|x\|^2} \in \text{Sym}_{m+1},$$

where Sym_{m+1} denotes the real symmetric $(m+1) \times (m+1)$ matrices. This mapping is invariant under nonzero rescaling of x , and therefore is well defined on projective space.

Let X be an \mathbb{RP}^m -valued random variable. In the single-coordinate case we consider the extrinsic mean matrix

$$K = \mathbb{E}[j_{\text{VW}}(X)].$$

Under a nonfocality condition, K has a unique largest eigenvalue λ_1 with eigenvector v_1 , and the corresponding axis $\pm v_1$ represents the VW extrinsic projective shape; see Patrangenaru and Ellingson [9].

In the case $q=1$, Fisher et al (1996)[5] showed that VW total-variance for PS is given by

$$t\Sigma_{\text{PS}} = 2(1 - \lambda_1).$$

Given a sample $\{X_i\}_{i=1}^n$ with homogeneous representatives $\{z_i\}_{i=1}^n \subset \mathbb{R}^{m+1} \setminus \{0\}$, we form

$$J_n = \frac{1}{n} \sum_{i=1}^n \frac{z_i z_i^\top}{\|z_i\|^2},$$

let $\lambda_1^{(n)}$ be the largest eigenvalue of J_n , and define the sample index

$$tS_{n,\text{PS}} = 2(1 - \lambda_1^{(n)}). \quad (10)$$

The hypothesis $H_0 : t\Sigma_{\text{PS}} = 0$ corresponds to the remaining landmark being projectively constant after frame normalization.

4 OPS Coplanarity Test and Asymptotic Standard Error

We now derive a delta-method based standard error for $tS_{n,\text{OPS}}$ and formulate a large-sample test for coplanarity in the OPS model.

4.1 Sample covariance and delta-method variance

Let $\{u_i\}_{i=1}^n \subset \mathbb{S}^m$ be OPS coordinates of a remaining landmark after oriented frame normalization. Define

$$\bar{u} = \frac{1}{n} \sum_{i=1}^n u_i, \quad R_n = \|\bar{u}\|, \quad tS_{n,\text{OPS}} = 2(1 - R_n).$$

We use the sample covariance matrix with $1/n$ normalization,

$$S_n = \frac{1}{n} \sum_{i=1}^n (u_i - \bar{u})(u_i - \bar{u})^\top.$$

Consider the smooth map $g : \mathbb{R}^{m+1} \rightarrow \mathbb{R}$ given by

$$g(x) = 2(1 - \|x\|).$$

Its gradient at \bar{u} is

$$\nabla g(\bar{u}) = -2 \frac{\bar{u}}{\|\bar{u}\|}.$$

Under standard moment and nondegeneracy assumptions, the central limit theorem and the delta-method yield

$$\sqrt{n}(tS_{n,\text{OPS}} - t\Sigma_{\text{OPS}}) \Rightarrow \mathcal{N}(0, \sigma_{\text{OPS}}^2),$$

with asymptotic variance

$$\sigma_{\text{OPS}}^2 = 4 \frac{\mu^\top \Sigma_{\text{E}} \mu}{\|\mu\|^2},$$

and empirical estimator

$$\widehat{\text{Var}}(tS_{n,\text{OPS}}) \approx \frac{1}{n} \nabla g(\bar{u})^\top S_n \nabla g(\bar{u}) = \frac{4}{n} \frac{\bar{u}^\top S_n \bar{u}}{\|\bar{u}\|^2}. \quad (11)$$

We write

$$\widehat{\text{SE}}_{\text{OPS}} = \sqrt{\widehat{\text{Var}}(tS_{n,\text{OPS}})} = \frac{2}{\sqrt{n}} \frac{\sqrt{\bar{u}^\top S_n \bar{u}}}{\|\bar{u}\|}. \quad (12)$$

This is the delta-method (extrinsic CLT-based) standard error used later in our numerical summaries.

We test coplanarity via the one-sided hypothesis

$$H_0 : t\Sigma_{\text{OPS}} = 0 \quad \text{vs.} \quad H_A : t\Sigma_{\text{OPS}} > 0. \quad (13)$$

For a nominal level $\alpha \in (0, 1)$, let $z_{1-\alpha/2}$ denote the standard normal quantile. A delta-method confidence interval for the population index $t\Sigma_{\text{OPS}}$ is

$$tS_{n,\text{OPS}} \pm z_{1-\alpha/2} \widehat{\text{SE}}_{\text{OPS}}. \quad (14)$$

Because the coplanarity hypothesis is one-sided, we test (13) by examining the lower endpoint of (14). At level α we reject H_0 if this lower endpoint is strictly positive.

Equivalently, we form the Z -statistic

$$Z_{\text{OPS}} = \frac{tS_{n,\text{OPS}}}{\widehat{\text{SE}}_{\text{OPS}}},$$

which is approximately standard normal under H_0 when dispersion is small. The associated one-sided p -value is $1 - \Phi(Z_{\text{OPS}})$.

As a complementary calibration we consider the scaled statistic

$$T_{\text{OPS}} = ntS_{n,\text{OPS}}$$

and compare it to a χ^2_2 reference when $m = 2$. In this planar single-coordinate case the OPS manifold has a two-dimensional tangent space at the extrinsic mean direction, which motivates the use of a chi-square distribution with two degrees of freedom as an asymptotic approximation for T_{OPS} .

4.2 Leave-out-outliers influence and reduced samples

In moderate size samples it is natural to examine the influence of individual scenes on $tS_{n,\text{OPS}}$. For $i = 1, \dots, n$ let $tS_{n,\text{OPS}}^{(-i)}$ be the OPS total-variance index computed after deleting scene i , and let $\widehat{\text{SE}}_{\text{OPS}}^{(-i)}$ be the corresponding standard error. The associated Z -statistics or the lower endpoints of the intervals (14) can be used to rank scenes by influence.

In the Sope Creek analysis we use a simple greedy scheme at a reference level $\alpha_{\text{ref}} = 0.05$: starting from the full sample, we remove the scene whose deletion yields the largest increase in the lower endpoint of the OPS interval at level α_{ref} . The process stops when this lower endpoint first becomes nonpositive. The remaining scenes form a reduced sample. We report both full-sample and reduced-sample statistics for OPS and PS, with the reduced sample defined by OPS.

4.3 Data and oriented projective frame

We now apply the OPS and PS total-variance indices to the Sope Creek stone, using the oriented projective frame $F = \{1, 2, 4, 3\}$.

The Sope Creek dataset consists of $n = 41$ photographs of a stone in a stream at Sope Creek, Marietta, GA [11]. Each image contains $k = 5$ landmarks placed at distinct, visually recognizable points on the stone's contour.

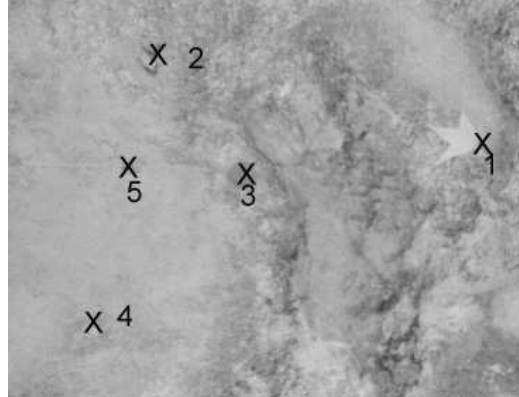


Figure 1: Landmarks for the Sope Creek stone: frame landmarks $\{1, 2, 4, 3\}$ and remaining landmark 5. Adapted from Figure 1.10 in Patrangenaru and Ellingson [9], originally due to Patrangenaru [11].

Following the projective shape literature, the aim is to assess whether the stone surface is projectively flat (coplanar) under central projection.

Throughout most of the analysis we use the oriented frame

$$F = \{1, 2, 4, 3\}, \quad R = \{5\},$$

so that landmarks 1, 2, 4, 3 form a projective frame and landmark 5 serves as the single remaining coordinate. For each scene i we form the 3×4 matrix P_i from the homogeneous

coordinates of the frame landmarks, compute a homography H_i mapping P_i to a canonical oriented frame $Q = [e_1, e_2, e_3, \mathbf{1}]$ (with $\mathbf{1} = (1, 1, 1)^\top$), and choose the representative H_i with $\det(H_i) > 0$. The oriented projective coordinate of landmark 5 in scene i is then

$$u_i = \frac{H_i \tilde{x}_{i,5}}{\|H_i \tilde{x}_{i,5}\|} \in \mathbb{S}^2, \quad i = 1, \dots, 41.$$

These unit vectors are the input to OPS analysis under the selected OP frame.

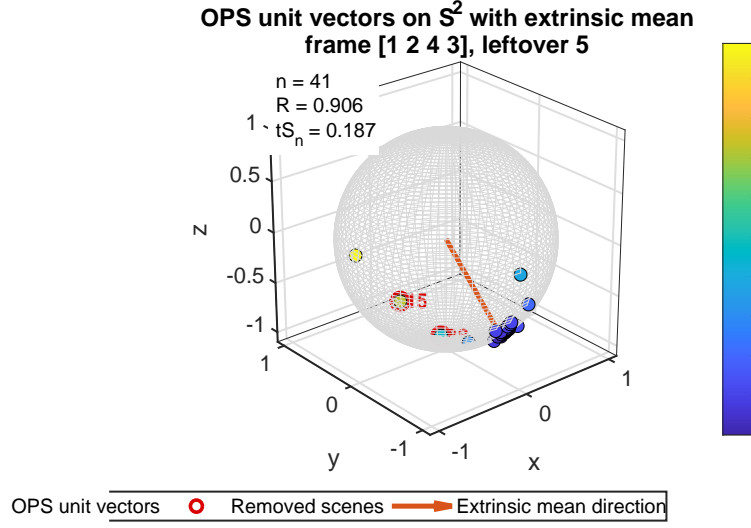
4.4 OPS geometry under the OP frame

Under the frame $F = \{1, 2, 4, 3\}$ the sample mean direction and mean resultant length are

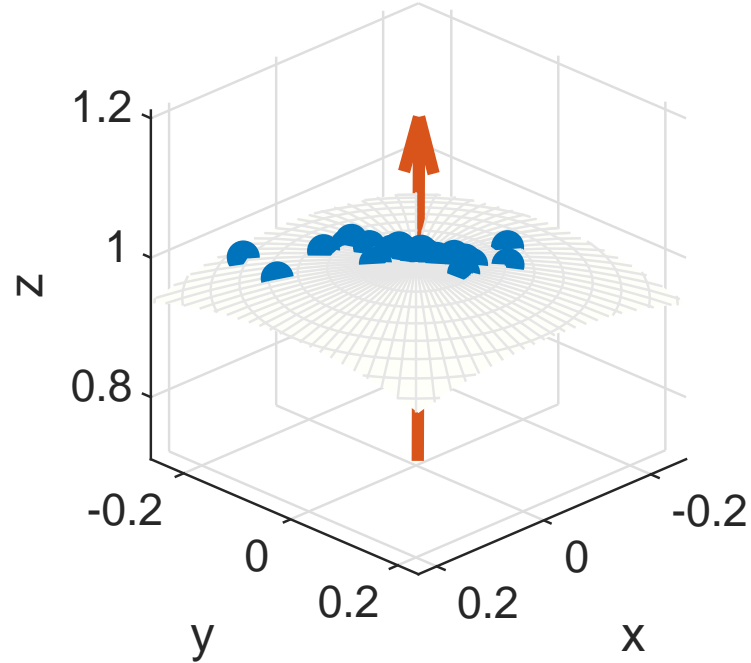
$$\bar{u} \approx (0.0073, -0.6720, -0.6082)^\top, \quad R_n \approx 0.9064.$$

Thus the oriented coordinates are tightly concentrated on a spherical cap of \mathbb{S}^2 pointing roughly toward the negative yz -hemisphere.

A natural method of visualization is to plot the OPS unit vectors $\{u_i\}$ on the sphere, with the extrinsic mean direction indicated by an arrow and influential scenes highlighted. In Figure 2 we show a full-sphere view together with a zoomed view that emphasizes the data cloud and the removed scenes under the primary frame choice.



(a) Full-sphere view under frame $\{1, 2, 4, 3\}$ with remaining landmark 5. The arrow shows the extrinsic mean direction and removed scenes are circled.



(b) Zoomed view near the extrinsic mean under the same frame, making the influential scenes easier to see.

Figure 2: OPS unit vectors on S^2 for the Sope Creek stone under frame $\{1, 2, 4, 3\}$ with remaining landmark 5: (a) full-sphere view; (b) zoomed view near the extrinsic mean.

The angular distances between u_i and the extrinsic mean $\hat{\mu}_E$ provide a one-dimensional summary of dispersion. Histograms of these angles, for the full and reduced samples, give a direct sense of how much the data tighten after removing influential scenes.

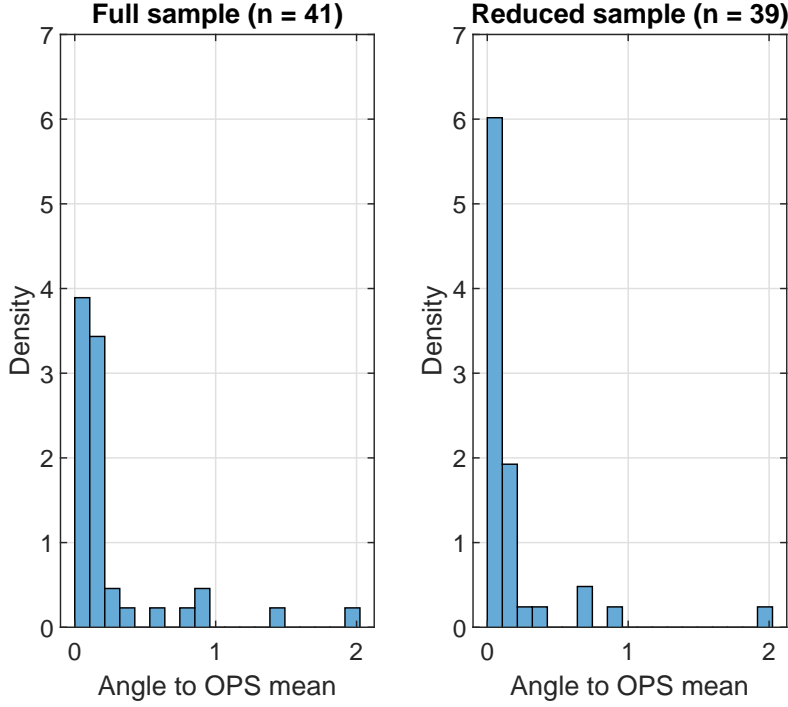


Figure 3: Angular distances between OPS unit vectors and the extrinsic mean under $F = \{1, 2, 4, 3\}$ for the full sample (left) and the OPS-based reduced sample (right).

4.5 Full-sample OPS under the OP frame

Using (9), the full-sample OPS total-variance index under F with $n = 41$ is

$$tS_{n,\text{OPS}} \approx 0.1871.$$

The scaled statistic is

$$T_{\text{OPS}} = ntS_{n,\text{OPS}} \approx 41 \times 0.1871 = 7.6731,$$

which yields a chi-square p -value

$$p_{\chi^2,\text{OPS}} \approx 0.0216$$

under a χ^2_2 reference.

From the sample covariance matrix S_n and (12) we obtain

$$\widehat{\text{SE}}_{\text{OPS}} \approx 0.0812.$$

The corresponding 95% delta-method confidence interval is

$$0.1871 \pm 1.96 \times 0.0812 = [0.028, 0.346].$$

The lower endpoint is strictly positive, so both the chi-square calibration and the normal approximation reject $H_0 : t\Sigma_{\text{OPS}} = 0$ at the 5% level in the full sample under the primary frame.

The corresponding delta-method standard error is about 0.076, leading to a 95% interval with a positive lower endpoint. Thus, under the primary frame F , the OPS detects a small but statistically significant deviation from perfect coplanarity in the full sample.

4.6 OPS-based reduced sample under the OP frame

Applying the OPS leave-one-out diagnostic of Section 4 with reference level $\alpha_{\text{ref}} = 0.05$ under the frame F identifies a pair of scenes with the largest influence on the lower endpoint of the OPS interval. Removing these two scenes yields a reduced sample of size $n_{\text{red}} = 39$.

On this reduced sample the OPS statistics under F become

$$R_n^{(\text{red})} \approx 0.9352, \quad tS_{n,\text{OPS}}^{(\text{red})} \approx 0.1297,$$

and

$$T_{\text{OPS}}^{(\text{red})} = 39 \times 0.1297 \approx 5.0581,$$

with chi-square p -value

$$p_{\chi^2,\text{OPS}}^{(\text{red})} \approx 0.0797.$$

The reduced-sample standard error $\widehat{\text{SE}}_{\text{OPS}}^{(\text{red})} \approx 0.0758$ yields a 95% interval

$$0.1297 \pm 1.96 \times 0.0758 = [-0.019, 0.278].$$

The lower endpoint is slightly negative, so at the 5% level the large sample one-sided OPS delta-method test no longer rejects $H_0 : t\Sigma_{\text{OPS}} = 0$ for the reduced sample under F . In this sense, after removing two influential scenes the OPS analysis under the primary frame is compatible with exact coplanarity, and with the results for concentrated PS coplanarity of Sope Creek stone data analysis in Patrangenaru(2001)[11], where on a reduced sample ($n = 37$) it was reported a total-variance estimate $\hat{t}_{n,I} \approx 0.58$ with standard error $\text{SE}(\hat{t}_{n,I}) \approx 2.63$, using inhomogeneous local coordinates, concluding that the coplanarity (flatness) hypothesis could not be rejected at $\alpha = 0.05$.

Our extrinsic OPS analysis, using a related frame ordering and an OPS-based removing two outliers to $n = 39$ under $F = \{1, 2, 4, 3\}$, reaches a qualitatively similar conclusion for the reduced samples: the oriented surface is compatible with coplanarity at the 5% level. At the same time, working on \mathbb{S}^2 provides a transparent “almost flat” geometry: the OPS index has the closed form $tS_{n,\text{OPS}} = 2(1 - R_n)$ with an interpretable delta-method standard error.

5 Acknowledgement and Discussion

The research in this manuscript was supported by the National Science Foundation under Grants DMS - 2311058 (Paige), DMS - 2311059 (Patrangenaru).

The OPS framework extends classical PS results by differentiating real scenes from their virtual images by means of orientation-preserving projective transformations. Within this framework, the OPS extrinsic total-variance index

$$tS_{n,\text{OPS}} = 2(1 - R_n), \quad R_n = \left\| \frac{1}{n} \sum_{i=1}^n u_i \right\|,$$

provides a simple scalar measure of dispersion of oriented projective coordinates around their extrinsic mean direction. It is expressed directly in terms of the mean resultant length on the sphere and fits naturally into the extrinsic Fréchet theory of Patrangenaru and Ellingson [9].

The Sope Creek analysis illustrates how OPS extrinsic total variance can be used in practice when a large sample of images of a 3D scene are available.

From a broader perspective, the OPS extrinsic total-variance index complements the OPS mean-based methods developed in Choi et al. [12]. Their work emphasizes OPS spaces and tests for differences in oriented mean shape, while the present contribution focuses on the magnitude of dispersion around a single OPS mean direction.

Note that for higher-dimensional scenes (such as $m = 3$), the OPS total-variance approach becomes difficult, due to the inability to observe the $m+2$ landmark as a convex combination of the previous ones. Finally, OPS total variance can be used in face recognition.

The table with corresponding landmark coordinates on Sope Creek stone data, from a sample of 41 images captured with a classical pinhole camera, and later digitized, can be found in Chapter 1 of Patrangenaru and Ellingson (2015)[9].

All computations described in this paper (including oriented projective alignment, construction of unit vectors on \mathbb{S}^2 , Veronese–Whitney covariance estimation) were carried out in MATLAB R2024b.

The scripts that generate the figures, tables, and numerical summaries reported in this paper are available from the authors upon request.

References

- [1] The MathWorks, Inc. *MATLAB*. Natick, Massachusetts, USA, 2024. Version R2024b.
- [2] J. Stolfi. *Oriented Projective Geometry: A Framework for Geometric Computations*. Academic Press, San Diego, CA, 1991.
- [3] R. Bhattacharya and V. Patrangenaru. Large sample theory of intrinsic and extrinsic sample means on manifolds. *Annals of Statistics*, 31(1):1–29, 2003.
- [4] R. Bhattacharya and V. Patrangenaru. Large sample theory of intrinsic and extrinsic sample means on manifolds, II. *Annals of Statistics*, 33(3):1225–1270, 2005.
- [5] Fisher, Nicholas I.; Hall, Peter; Jing, Bing-Yi; Wood, Andrew T. A. Improved pivotal methods for constructing confidence regions with directional data. *J. Amer. Statist. Assoc.* 91 (1996), no. 435, 1062–1070
- [6] K. V. Mardia and V. Patrangenaru. Directions and projective shapes. *Annals of Statistics*, 33(4):1666–1699, 2005.
- [7] R. Bhattacharya and L. Lin. Omnibus central limit theorem for Fréchet means and nonparametric inference on non-Euclidean spaces. *Proceedings of the American Mathematical Society*, 145(1):413–428, 2017.
- [8] V. Balan, M. Crane, V. Patrangenaru, and X. Liu. Projective shape manifolds and coplanarity of landmark configurations: A nonparametric approach. *Balkan Journal of Geometry and Its Applications*, 14(1):1–10, 2009.
- [9] V. Patrangenaru and L. Ellingson. *Nonparametric Statistics on Manifolds and Their Applications to Object Data Analysis*. CRC Press, Boca Raton, FL, 2015.
- [10] I. L. Dryden and K. V. Mardia. *Statistical Shape Analysis: With Applications in R*, 2nd ed. John Wiley & Sons, Chichester, UK, 2016.
- [11] V. Patrangenaru. New large sample and bootstrap methods on shape spaces in high level analysis of natural images. *Communications in Statistics – Theory and Methods*, 30(8–9):1675–1693, 2001.
- [12] S. Choi, R. L. Paige, and V. Patrangenaru. Oriented projective shape analysis. *BSG Proceedings*, 29:1–11, 2022.
- [13] J. Stolfi, *Oriented Projective Geometry*, Academic Press, 1991.